Toxicology 285 (2011) 72–80

Contents lists available at ScienceDirect

Toxicology

journal homepage: www.elsevier.com/locate/toxicol

16-Hydroxycleroda-3,13-dien-15,16-olide deregulates PI3K and Aurora B activities that involve in cancer cell apoptosis

Yi-Hsiung Lin[a], Chien-Chih Lee[a], Wen-Li Chan[b], Wen-Hsin Chang[c], Yang-Chang Wu[a,d,e,*], Jan-Gowth Chang[f,g,h,i,**]

[a] Graduate Institute of Natural Products, College of Pharmacy, Kaohsiung Medical University, Kaohsiung, Taiwan
[b] Department of Biological Science and Technology, Institute of Bioinformatics, National Chiao Tung University, Hsinchu, Taiwan
[c] Graduate Institute of Medicine, College of Medicine, Kaohsiung Medical University, Kaohsiung, Taiwan
[d] Graduate Institute of Integrated Medicine, College of Chinese Medicine, China Medical University, Taichung, Taiwan
[e] Natural Medicinal Products Research Center, China Medical University Hospital, Taichung, Taiwan
[f] Institute of Clinical Medicine, College of Medicine, Kaohsiung Medical University, Kaohsiung, Taiwan
[g] Center of Excellence for Environmental Medicine, Kaohsiung Medical University Hospital, Kaohsiung, Taiwan
[h] Cancer Center, Kaohsiung Medical University Hospital, Kaohsiung, Taiwan
[i] Department of Laboratory Medicine, Kaohsiung Medical University Hospital, Kaohsiung, Taiwan

ARTICLE INFO

Article history:
Received 11 January 2011
Received in revised form 7 April 2011
Accepted 8 April 2011
Available online 19 April 2011

Keywords:
16-Hydroxycleroda-3,13-dien-15,16-olide
Aurora B
PI3K
Mitotic block
Apoptosis

ABSTRACT

The PI3K-AKT pathway and Aurora kinase play essential roles in such cellular processes as cell survival, angiogenesis, and differentiation, and are usually expressed at maximum levels during cancer cell proliferation. The present study investigated the effect of the natural compound, 16-hydroxycleroda-3,13-dien-15,16-olide (PL3), on regulating the PI3K-AKT pathway and Aurora B, which led to cancer cell apoptosis. PL3 acts as a PI3K inhibitor by influencing cell survival, signaling transduction, and cell cycle progression. It was observed that PL3 targeted and induced dephosphorylation of the PI3K pathway, degradation of Aurora B and mitotic-related gene expressions, and sequentially shut down the cell cycle. This eventually resulted in cell death. As Aurora B was downregulated, spindle dysfunction and destruction of the G_2/M phase checkpoint resulted in DNA-damaged cells undergoing apoptosis. Moreover, PL3 also resensitized T315I-mutated Bcr-ABL$^+$ BA/F3 cells to improve the cytotoxicity of Imatinib in Imatinib-resistant cell line. Taken together, PL3 can perturb the PI3K-AKT pathway and Aurora B resulting in gene silencing and cell cycle disturbance. It was demonstrated that PL3 acted like a novel small-molecule PI3K modulator, thereby potentially contributing to cancer chemotherapy and combination medication.

1. Introduction

The Aurora family can be classified into three members, Aurora A, B, and C, which are essential for cell-cycle regulation. The family also has serine/threonine kinase activity which modifies microtubes during chromosome movement and segregation. Aurora A is localized in centrosomes and is important for maturation, spindle assembly, and metaphase I spindle orientation. Aurora B is localized to microtubules near kinetochores, which are highly expressed and play key roles in ensuring the genetic stability of cell division (Gully et al., 2010). Chromosome segregation is a critical step in maintaining gene stability, and the overexpression of Aurora B is required to coordinate cellular process (Schmitt et al., 2002). Anticancer reagents can kill cells by destroying the spindle checkpoint integrity.

It is known that PI3K-AKT and Aurora kinases are important targets for interventions by cancer therapies, and scientists recently found cross-talk between the PI3K-AKT pathway and Aurora kinase activation (Liu et al., 2008; Yao et al., 2009). Phosphatidylinositol (PI) 3-kinases (PI3Ks) are now well-known as important regulators of cell survival, differentiation, angiogenesis, cell invasion, and metastasis (Kim and Chung, 2002). They were found to be activated during colony stimulating factor (CSF)-1-mediated cell proliferation and survival, and required for prevention of apoptosis in various types of cells by regulating growth factors (Scheid et al.,

Abbreviations: PL3, 16-hydroxycleroda-3,13-dien-15,16-olide; APK, mitogen-activated protein kinases; CPC, chromosomal passenger complex; INCENP, inner centromere protein.

* Corresponding author at: Graduate Institute of Integrated Medicine, College of Chinese Medicine, China Medical University, No. 91, Hsueh-Shih Road, Taichung 40402, Taiwan. Tel.: +886 4 22053366.
** Corresponding author at: Institute of Clinical Medicine, College of Medicine, Kaohsiung Medical University, No. 100, Shih-Chuan 1st Road, Kaohsiung 807, Taiwan. Tel.: +886 7 312 1101.
E-mail address: jgchang@ms.kmuh.org.tw (J.-G. Chang).

0300-483X/$ – see front matter © 2011 Elsevier Ireland Ltd. All rights reserved.
doi:10.1016/j.tox.2011.04.004

1995; Takashima et al., 1996; Varticovski et al., 1989). There are three classes of PI3Ks, classes I, II, and III with regulatory subunits for each according to their respective structural characteristics and substrate specificity (Fruman et al., 1998; Liu et al., 2009). Class I PI3K is the most commonly studied, and is directly activated by cell surface receptors (Fruman et al., 1998). The serine/threonine kinase AKT was identified as having a crucial role amongst PI3Ks and preventing apoptosis by targeting Bad, caspase-9 and Forkhead transcription factors. Both phosphorylation events on T308 and S473 are required for full activation of AKT (Alessi et al., 1997). Activated AKT is initially translocated to plasma membranes, and has the capacity to phosphorylate a variety of substrate proteins in order to perform its functions in cells, which are involved in apoptosis signaling transduction (Alessi et al., 1996; Engelman et al., 2006).

A wide variety of natural compounds are toxic to cancer cells, but their mechanisms of toxicity differ. 16-Hydroxycleroda-3,13-dien-15,16-olide (PL3), one of the major clerodane diterpenoid compounds isolated from the bark of *Polyalthia longifolia*, was reported to exhibit anti-inflammatory activity against fMLP/CB-induced superoxide generation by neutrophils. In addition to the anti-inflammatory effect, it also showed cytotoxicity towards breast cancer cells and hepatoma carcinoma cells (Chang et al., 2006; Shih et al., 2010). In a previous study, 22 compounds were isolated from *P. longifolia* (Chang et al., 2006). Increasingly, cytotoxic diterpenes were isolated from this plant. However, the mechanism of action of these treasured chemicals against cancer is still unclear. In the present study, the effects of PL3 on various cancer cell lines were investigated, and its possible molecular mechanism of apoptosis was determined.

2. Materials and methods

2.1. Chemicals

RPMI 1640 medium, Dulbecco's modified Eagle's medium (DMEM), fetal calf serum (FCS), trypan blue, penicillin G, and streptomycin were obtained from Gibco BRL (Gaithersburg, MD, USA). 3-(4,5-Dimethylthiazol-2-yl)-2,5-diphenyltetrazolium bromide (MTT), dimethyl sulfoxide (DMSO), ribonuclease (RNase), and propidium iodide (PI) were purchased from Sigma–Aldrich (St. Louis, MO, USA). The antibodies against histone H3, caspase-3, phospho-P85, P85, phospho-AKT, and AKT were purchased from Cell Signaling (Danvers, MA, USA). The antibodies for phospho-H3S10, and pro-caspase-9 were purchased from ABcam (Cambridge, MA, USA). The antibodies for phospho-JNK, JNK, Aurora-B, cyclin A, cyclin B, Cdk1, and Cdk2 were obtained from BD Biosciences (San Jose, CA, USA). The antibody for β-actin was obtained from Chemicon (Temecula, CA, USA), and the anti-mouse and anti-rabbit IgG peroxidase-conjugated secondary antibodies were purchased from Pierce (Rockford, IL, USA). Anti-PARP and XIAP were purchased from Santa Cruz Biotechnology (Santa Cruz, CA, USA), and the Hybond ECL transfer membrane and enhanced chemiluminescence (ECL) Western blotting detection kit were obtained from Amersham Life Science (Buckinghamshire, UK). PL3 was isolated from *P. longifolia*, as previously described (Chang et al., 2006). LY294002, wortmannin, and SP600215 were purchased form Sigma (St. Louis, MO, USA). PL3 was dissolved in DMSO (<0.01%) immediately prior to the experiments.

2.2. Cell culture

Human leukemia K562, HL-60, and Molt-4 cells, colon cancer SW620 cells, lung cancer A549 cells, and brain cancer GBM8401 cells were obtained from the Food Industry Research and Development Institute (Hsinchu, Taiwan). The BA/F3 transfectant (expressing the T315I mutant, Bcr-ABL$^+$) cell line was provided by Michael W. Deininger. Cells were maintained in RPMI 1640 medium (leukemia cell lines) and DMEM (solid-tumor cell lines) supplemented with 10% FBS, 2 mM glutamine, and antibiotics (100 U/ml penicillin and 100 μg/ml streptomycin) at 37 °C in a humidified atmosphere of 5% CO_2.

2.3. Cell viability inhibition assay

The viability of cells was determined by the trypan blue dye exclusion method and assessed by the MTT assay. The exponentially growing cells (1×10^4) were plated in 96-well plates and treated with a series of concentrations of PL3 after 24 h of growth. Incubation was carried out at 37 °C for 72 h. Cells exposed to 0.2% trypan blue were counted in a hemocytometer. The MTT solution was added to each well (1.2 mg/ml) and incubated for 4 h. Cell survival was assessed by measuring the absorbance at 570 nm in an ELISA plate reader.

2.4. Flow cytometric analysis

The control and treated cells were harvested, washed in cold phosphate-buffered saline (PBS), fixed in 70% ethanol, and stored at 4 °C. Before the analysis, DNA was treated with an RNase-A solution (500 U/ml) at 37 °C for 15 min and stained with PI (50 μg/ml) in 1.12% sodium citrate at room temperature. The DNA content was determined by a flow cytometric analysis with a Coulter EPICS XL Flow Cytometer (Coulter, Miami, FL, USA). The fractions of cells in the G_0/G_1, S, and G_2/M phases were analyzed using cell cycle analysis software, Multicycle (Phoenix Flow System, San Diego, CA, USA).

2.5. Western blot analysis

Western blotting was used to analyze the protein expression of the treated cells. The cells were harvested and extracted using lysis buffer (50 mM Tris–HCl (pH 7.5), 137 mM sodium chloride, 1 mM EDTA, 1% Nonidet P-40, 10% glycerol, 0.1 mM sodium orthovanadate, 10 mM sodium pyrophosphate, 20 mM β-glycerophosphate, 50 mM sodium fluoride, 1 mM phenylmethylsulfonyl fluoride, 2 μM leupeptin, and 2 μg/ml aprotinin). The lysates were centrifuged at 20,000 × *g* for 30 min, and the protein concentration in the supernatant was determined with a BSA protein assay kit (Pierce, Rockford, IL, USA). Equal amounts of proteins were separated by sodium dodecylsulfate (SDS)-polyacrylamide (10%) gel electrophoresis (PAGE) and then were electrotransferred to a polyvinylidene difluoride (PVDF) membrane. The membrane was blocked with a solution containing 5% nonfat dry milk in TBST buffer (20 mM Tris–HCl (pH 7.4), 150 mM NaCl, and 0.1% Tween 20) for 1 h and washed with TBST buffer. The indicated primary antibodies were incubated, washed, and monitored by immunoblotting by using specific antibodies. These proteins were detected by ECL.

2.6. Total RNA extraction and complementary cDNA reverse transcription for a real-time PCR analysis

After PL3 treatment, mRNA was extracted from cells using a TurboCapture 8 mRNA kit (Qiagen, Chatsworth, CA, USA) according to manufacturer's instructions. Reverse transcription of the mRNA was performed using a mixture of oligo(dT), random primers, and Moloney murine leukemia virus reverse transcriptase (Promega, Madison, WI, USA). To quantify the RNA expression, a real-time PCR was performed in a final volume of 20 μl using the LightCycler instrument (Roche Diagnostics) according to manufacturer's recommendations. Primers specific for humans were designed using the ProbeFinder software (Roche, Taiwan) and synthesized by custom oligonucleotide synthesis (Biossom, Taiwan). The primer sequences used in this study are in Table 1. The conditions for cDNA amplification were as follows: 40 cycles of 95 °C for 1 s (denaturation), followed by 60 °C for 10 s (annealing), and 72 °C for 30 s (extension). At the end of every cycle, the fluorescence of each sample was measured at 88 °C to allow specific quantification of the real-time PCR product (Rakvag et al., 2005).

The original data of the real-time PCR product quantifications for each group were normalized to the respective mean RNA expressions of the three housekeeping genes (ALAS1, HMBS, and GAPDH) determined for the respective cDNA pool. The

Table 1
Primer list.

Name	Forward primer	Reverse primer
IKKa	tgtgcctcttctagcaatgga	ttctggtttgttgagcagctt
BAX	atgttttctgacggcaacttc	atcagttccggcaccttg
BAD	accagcagcagccatcat	ggtaggagctgtggcgact
P27	gccaaagtgaacagcatcag	tcatcatccacttgcagacc
MYT1	gaccccgagctgatgaagt	cgtatttcccgctgatgtg
TSC1	caaccagagccaggaattaca	cagctccgcaatcatgttc
FOXO3	cttcaaggataagggcgaca	cgactatgcagtgacaggttg
FOXO4	cgagggactggacttcaact	ggctcaagggtaaagagtagatatga
BUB1	tgctctttggcacttacatga	ccacatatccaaatgaggaagc
BUB3	aatgctgggaccttctctca	tccgtaagtcccacaccaac
BUB1B	cagtcagactctcagcatcaaga	cgaggcagaagaaccagaga
CENPA	agcttcagaagagcacacacc	aggcgtcctcaaagagatga
CENPC1	catctgattggtgggtggtaa	ggctactattgtgatgcattgg
CENPF	gagtcctccaaaccaacagc	tccgctgagcaactttgac
CENPL	cggaagcatttcttgtcca	gttgcagtcaaccaagatcg
CENPM	aacacggccaccatcttg	gggactttgccaagtggac
CENPN	cagactccgtacgccttcac	ggtccattttcacaatctgatg
MAD2L1	cagatcacagctacggtgaca	tctgtataaatcagcagatcaaatgaa
APC	gcatggaccaggacaaaaat	gaacacacacagcaggacagat
CDC2	tccatggatctgaagaaatacttg	accttaacaagtgaagaatccatgt
CDC25A	atctcttcacacagaggcagaa	ccctggttcactgctatctctt

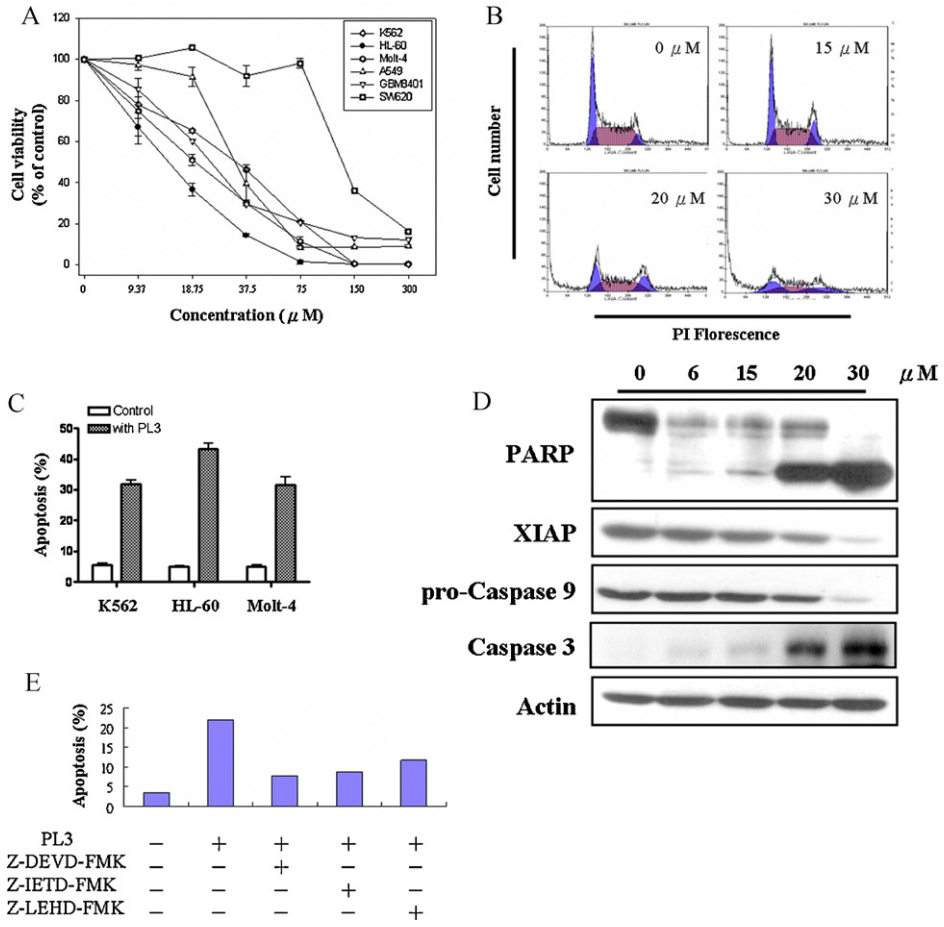

Fig. 1. PL3 induces cytotoxicity and apoptosis in cancer cells. (A) Leukemia K562, HL-60, Molt-4, SW620, HT29, GBM8401, and A549 tumor cell lines were treated with various concentrations (0–300 μM) of PL3, cell viability was detected by an MTT assay, and IC_{50} values were calculated. (B) K562 cells were treated with the indicated concentrations (0, 15, 20, and 30 μM) of PL3 for 24 h, and the cell-cycle distribution was analyzed by flow cytometry and propidium iodide (PI) staining. (C) Leukemia cell lines were treated with each IC_{50} concentration for 24 h, then apoptotic bodies were determined by PI staining and flow cytometry. (D) K562 cells were treated with 0–30 μM PL3 for 24 h, and whole-cell lysates were used to analyze the expressions of pro-caspase-9, activated caspase-3, XIAP, and the total/cleavage form of PARP after treatment. (E) K562 cells were pretreated with 10 μM of the individual caspase inhibitors of Z-DEVD-FMK, Z-IETD-FMK, and Z-LEHD-FMK for 1 h, and then they were treated with 20 μM PL3 for 24 h to determine the level of apoptosis by flow cytometry and PI staining.

resulting quantitative differences represented the relative changes in RNA expression amongst the experimental groups.

2.7. Immunofluorescence microscopy

Assessment of Aurora B distribution in K562 cell line was performed employing immunofluorescence techniques, by incubating PL3-treated cells in the presence of a primary monoclonal antibody against Aurora B, followed by incubation with an Alexa 594-conjugated (ex 594 nm/em 618 nm) secondary antibody. The section was added by DAPI (4′,6-diamidino-2-phenylindole) to identify the nucleus and performed on a Leica immunofluorescence microscopy. The samples were pretreated by 0.54% KCl and fixed by acetic acid–methanol mixture (3:1) on glass slides. Fluorescent cells spectral images were captured with a SD200 SpectraCube system (Applied Spectral Imaging, Migdal Ha'Emek, Israel) mounted on a Leica microscope (Leica, Wetzlar, Germany). Digital images were optimized for image resolution (final resolution 300 dpi), brightness, and contrast using Adobe Photoshop 7.0 (Adobe Systems, San Jose, CA). Images were not altered in any way, e.g., by removing or adding image details.

2.8. Molecular modeling and docking

The docking of PL3 into the binding site of the PI3K protein was explored using iGEMDOCK v2.1 (Generic Evolutionary Method for molecular Docking) (Yang and Chen, 2004) software, which was a program for computing a ligand conformation and orientation relative to the active site of the target protein. To validate the molecular modeling programs, the docking accuracy of GEMDOCK was first evaluated by docking three known PI3K inhibitors, wortmannin, triciribine and LY294002 into the binding site (Arcaro and Wymann, 1993; Dieterle et al., 2009; Gharbi et al., 2007; Yano et al., 1993). The 3D structure of compounds was prepared by ACD/ChemSketch (Osterberg and Norinder, 2001). The binding pocket of the PI3K was defined to include the amino acid residues within an 8 Å radius sphere centered around the binding site of LY294002. In the present study, the GEMDOCK parameters included the population size (n = 500), generations (g = 80) and number of solutions (s = 10). Finally, the docked poses were clustered according to the interaction profiles.Statistical analysis

All the obtained experimental results were reproduced in at least three independent experiments. Differences between the treatment and control were analyzed by the Student's t-test. A probability of $p < 0.05$ was considered significant.

3. Results

3.1. PL3 induces apoptotic cell death and interferes with the cell-cycle distribution

We first determined the effect of PL3 by focusing on leukemia K562 cells. Other types of cancer cells, HL-60 and Molt-4 cells, and solid-tumor SW620, A549, and GBM8401 cells were used. These cell types are representative models for leukemia, colon and lung cancer, and brain malignant glioma, and were used to further confirm PL3 cytotoxicity against tumor cells. Cells were incubated with 0–300 μM of PL3 for 24 h, and then an MTT assay was used to analyze cell viability. After 24 h of exposure, significant decreases in cell viabilities were observed following an increased concentration of PL3 treatment (Fig. 1A). PL3 exhibited greater toxicity in leukemia cells (with IC_{50} values of about 15, 20, and 30 μM for HL-60,

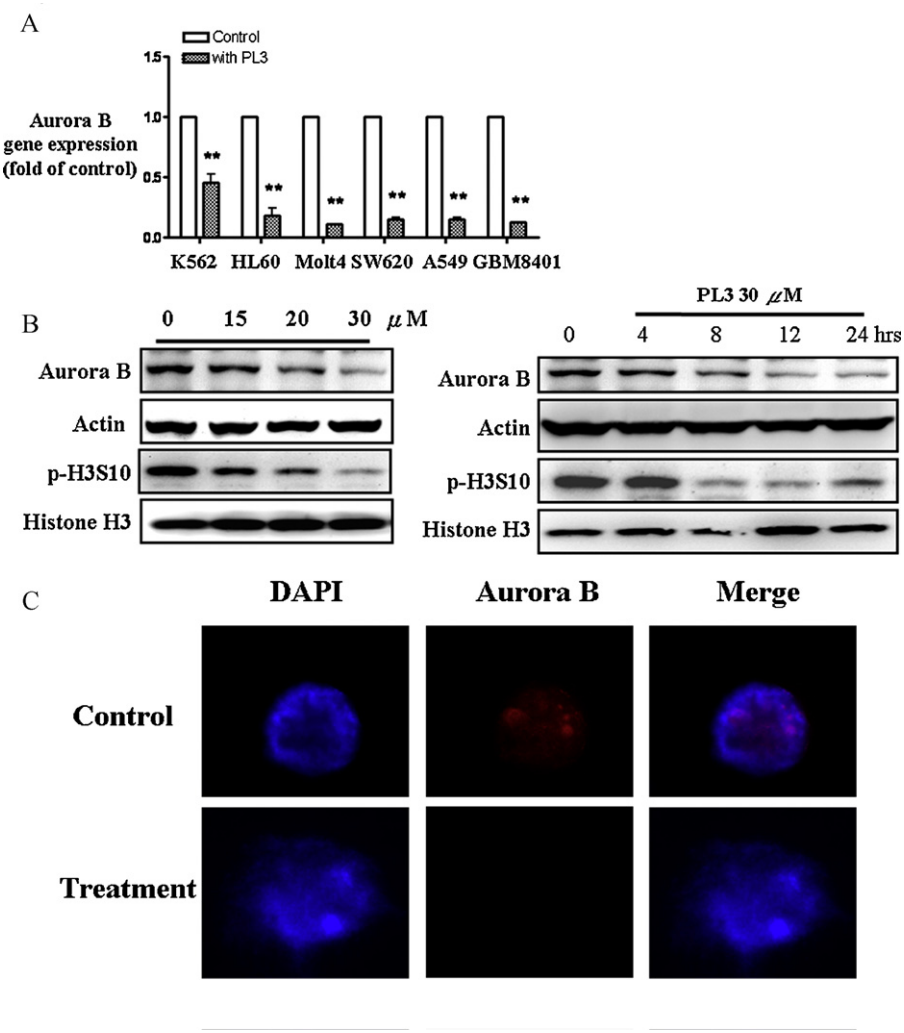

Fig. 2. PL3 inhibits Aurora B expression and histone H3 dephosphorylation. (A) K562, SW620, A549, and GBM8401 cells were each treated with the respective IC_{50} values of PL3 for 24 h, and Aurora B gene expression was analyzed by a real-time PCR. (B) K562 cells were treated with various concentrations (0–30 μM) of PL3 for 24 h and 30 μM for the indicated times (0–24 h), and Aurora B protein expressions and the phosphorylation status of histone H3 Ser10 were analyzed by Western blotting. (C) K562 cells were treated with or without 30 μM of PL3 for 24 h, and then stained with DAPI and an Aurora B antibody. The cell morphology and Aurora B distribution were examined using fluorescence microscopy. $^{*}p < 0.05$; $^{**}p < 0.01$ (*t*-test).

Molt-4, and K562 cells; and 140, 35, and 20 μM for SW620, A549, and GBM8401 cells, respectively; Fig. 1A). The cell-cycle distribution of K562 cells with PL3 treatment was determined by flow cytometry (Fig. 1B). The sub-G_1 generations in the three leukemia cell lines increased in dose-dependent manners (Fig. 1C). The results showed that PL3 disturbed the cell-cycle process and induced leukemia cell death through an increase in the sub-G_1 phase. Western blotting was performed to examine the impact of PL3 on apoptosis signaling transduction. K562 cells were treated with the indicated concentrations of PL3 and incubated for 24 h. It was observed that PL3 induced cleavage of procaspases-9 and -3, converted them into their active forms, and reduced XIAP protein expression in K562 cells. With activation of caspase-3, cleavage of PARP, its downstream DNA repair protein, was detected (Fig. 1D).

Table 2
The features of docked poses by GEMDOCK.

Compound	Energy	VDW	HBond
PL3	−113.36	−94.7	−18.66
Wortmannin	−114.9	−97.1	−17.8
Triciribine	−111.48	−82.21	−29.27
LY294002	−88.61	−82.5	−6.11

VDW, van der Waals.

Moreover, respective inhibitors of caspases-3, -8, and -9 of Z-DEVD-FMK (10 μM), Z-IETD-FMK (10 μM), and Z-LEHD-FMK (10 μM) were used to determine the role of caspases in PL3-induced apoptosis. K562 cells were pretreated with or without the individual caspase inhibitors for 1 h and then treated with 30 μM PL3 for 24 h. In the experiment, the apoptosis-inducing ability of PL3 was reduced by more than 64% by Z-DEVD-FMK, 60% by Z-IETD-FMK, and 50% by Z-LEHD-FMK. These results suggest that PL3 induces apoptosis by activating both the extrinsic and intrinsic pathways (Fig. 1E). We further tested the apoptosis-inducing effect of PL3 in another three cell lines to investigate its molecular mechanism. In dose-dependent manners, treatment concentrations of PL3 used with SW620 cells were 50, 100, and 150 μM; 10, 20, and 35 μM with A549 cells; and 7, 14, and 20 μM with GBM8401 cells. Similar results of PARP cleavage and caspase-3 activation were observed in SW620 and GBM8401, but not in A549, cells (Supplementary Fig. S1).

3.2. Aurora B expression and histone H3 dephosphorylation induced by PL3

Given the importance of the Aurora B kinase in cancer cell mitosis and metastasis, its expression was examined. As shown in

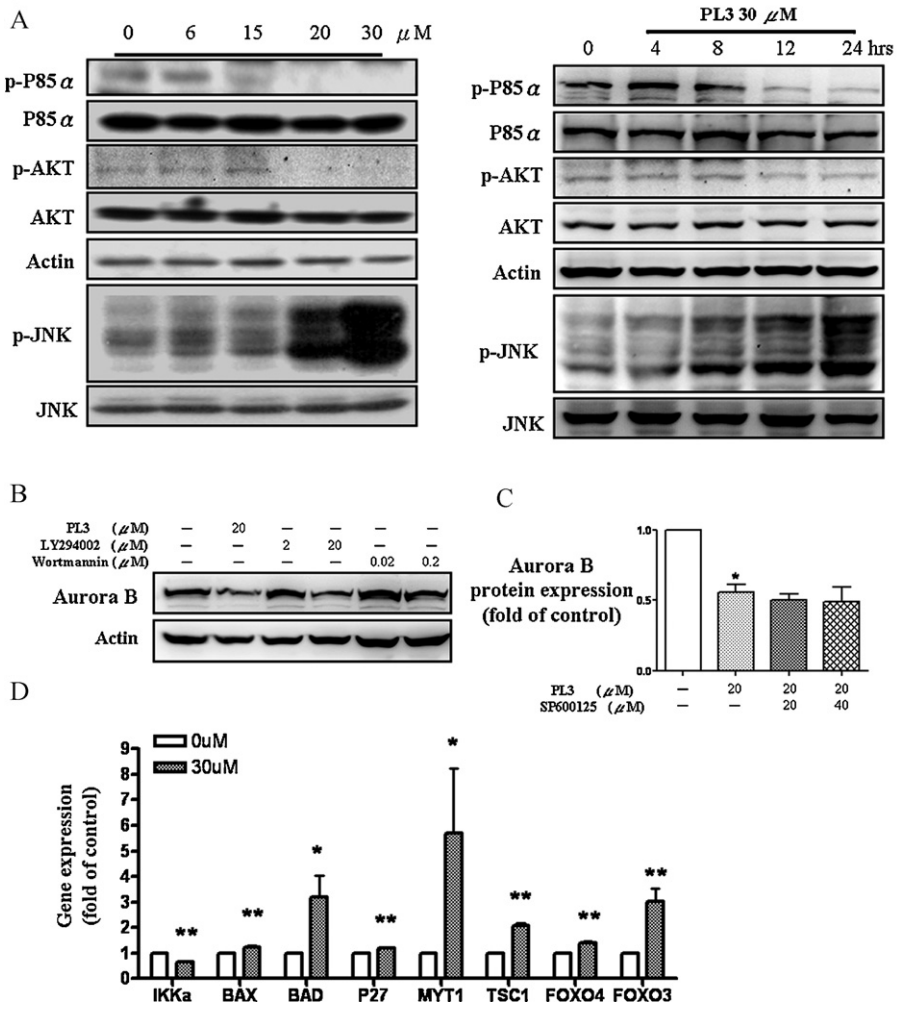

Fig. 3. PL3 inhibits cell survival-signaling transduction and upregulates downstream activation. (A) The PI3K-AKT pathway was inactivated through the dephosphorylation and activation of JNK induced by PL3 at the indicated concentrations for 24 h and 30 μM of PL3 for time-dependent treatment. K562 cells were prepared for a Western blot analysis. (B) K562 cells were individually treated with PL3 (20 μM), LY294002 (2 and 20 μM), and wortmannin (0.02 and 0.2 μM) for 24 h and harvested to analyze Aurora B protein expression. (C) PI3K-AKT downstream effectors in the presence or absence of PL3-treated K562 cells were determined by a real-time PCR. $^{*}p < 0.05$; $^{**}p < 0.01$ (*t*-test).

Fig. 2A, we found that PL3 inhibited Aurora B gene expression in all six cell lines compared to untreated cells. With the reduction of Aurora B in gene level, the protein expression was determined later. Through a Western blot analysis, it was found that PL3 decreased Aurora B protein in both dose- and time-dependent manners in K562 cells. Furthermore, with the decay of Aurora B expression, there was also a reduction in the phosphorylation status of the histone H3 Ser10 (H3S10) (Fig. 2B). PL3 induced the same reductions in Aurora B and the phosphorylation status of H3S10 in the other three solid tumor cell lines (Supplementary Fig. S2). Immunofluorescence was performed to evaluate the distribution of Aurora B in PL3-treated K562 cells. Aurora B expression was not observed in cells treated with PL3, while control cells expressed a normal Aurora B distribution (Fig. 2C).

3.3. PL3 inhibits PI3K activity and its effect on downstream signal regulation

According to the regulation by PL3 of Aurora B expression, the effect of PL3 on Aurora B's upstream regulator, the PI3K-AKT pathway, was further examined. The PI3K-AKT pathway is critical for the inhibition of apoptosis, and the AKT pathway is vital for cell survival. In Fig. 3A, significant reductions were obtained in the PI3K subunits, phospho-P85α and phospho-AKT, after PL3 treatment. With reductions in upstream PI3K-AKT phosphorylation, an increase in phosphorylation of the downstream apoptosis-inducer, JNK, was detected. We further confirmed these regulatory effects of PL3 in the other three tested cell lines. It was found that PL3 reduced PI3K-AKT pathway activities and activated JNK in all of them (Supplementary Fig. S3). The inhibitory effects of the PI3K inhibitors, LY294002 and wortmannin, on Aurora B expression were further tested to confirm the cross-regulation between these two essential pathways. K562 cells were individually treated with PL3 (20 μM), Ly249002 (2 and 20 μM), and wortmannin (0.02 and 0.2 μM) for 24 h and harvested for Aurora B expression. It was observed that LY294002 had a similar effect on reducing Aurora B expression as PL3 (Fig. 3B). Moreover, the effect of the JNK inhibitor, SP600125, on Aurora B expression was investigated to determine the role of JNK in the overall process of Aurora B decreased. As shown in Fig. 3C, it was found that there was no significant change in Aurora B protein expression after co-treatment with SP600125 (20, 40 μM) and PL3 (20 μM). As the PI3K-AKT pathway is well studied in apoptosis prevention, and in consideration of the inhibitory effect of PL3 on the pathway, gene expressions of proapoptotic effectors were determined. K562 was treated with 30 μM PL3 or left untreated for 24 h. A real-time PCR was used for the gene expression analysis. Fig. 3D shows that BAD significantly increased in PL3-treated K562 cells by 3-fold compared to the control. In addition,

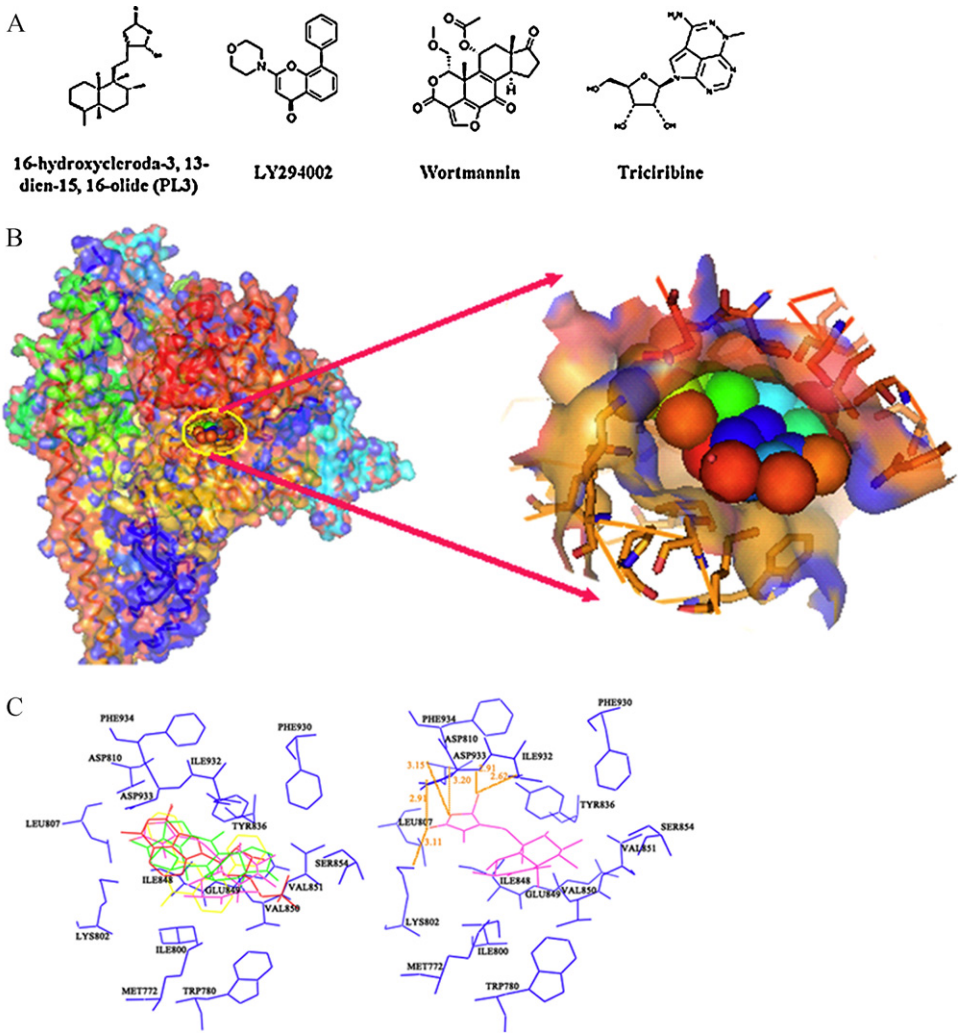

Fig. 4. Molecular model of the interaction between PL3 and PI3K P85α. (A) Chemical structures of wortmannin, triciribine, LY294002, and PL3. (B) Docked model of the PI3Kα-PL3 complex. The surface of PI3Kα with the PL3 molecule drawn in by van der Waals forces (left). The docked region is circled in yellow and expanded in a close-up on the right. (C) Docked conformations of wortmannin (green), triciribine (red), LY294002 (yellow), and PL3 (pink) in PI3Kα with the lowest scores were compared to the crystal structures based on the root-mean-square deviation (RMSD) of heavy atoms (left). The main contract residues (blue) of PI3Kα were labeled, and hydrogen bond distances (dashed with orange line) between PL3 were calculated (left). (For interpretation of the references to color in this figure legend, the reader is referred to the web version of the article.)

similar increased expressions of the proapoptotic genes, MYT1, TSC1, FoxO3, and FoxO4, were also determined in the presence of PL3 treatment, thereby suggesting that the PI3K-AKT downstream tumor-suppressor and proapoptotic gene expressions were activated by PL3 treatment.

3.4. Virtual screening for PI3K inhibitors

The binding affinity of PL3 towards the PI3K protein was investigated because of the inhibitory effect of PL3 on the PI3K-AKT pathway. iGEMDOCK was employed to predict the docked conformations of wortmannin, triciribine, LY294002, and PL3 in the binding cavity of PI3Kα based on calculated values of binding energies. The chemical structures and features of the docked poses are shown in Fig. 4A and Table 2, respectively. The surface of PI3Kα with a PL3 molecule drawn by van der Waals forces is shown in Fig. 4B. It was observed that the PL3 molecule was located in the hole of PI3Kα. The docked region is circled in yellow and expanded in a close-up (right). Fig. 4C (left) also shows the docked conformations of wortmannin (green), triciribine (red), LY294002 (yellow), and PL3 (pink) in PI3Kα with the lowest scores compared to the crystal structures based on the root-mean-square deviation (RMSD) of the heavy atoms. The main contract residues (blue) of PI3Kα were labeled, and hydrogen bond distances (dashed with orange line) between PL3 (Fig. 4C) were calculated. The residues of LYS802, ASP810, TYR836, and ASP933 were highly conserved in all of the chemical compounds. However, LY294002 was excluded. According to GEMDOCK, the respective energies of wortmannin, triciribine, LY294002, and PL3 were −114.9, −111.5, 88.6, and 113.4 kcal/mol.

3.5. PL3 treatment inhibits cell spindle checkpoint-associated gene expression and causes G_2/M phase arrest

PL3 exhibited an inhibitory effect on cell-cycle progression. The impact of PL3 on cell-cycle arrest and spindle checkpoint-associated gene expressions was investigated. It was observed that PL3 induced cell-cycle arrest in the G_2/M phase as the G_2/M percentage increased from 7% to 27% after exposure (Fig. 5A). Cyclin–Cdk complex expressions were examined to determine the effect of PL3 on cell-cycle checkpoint-related proteins. It was evident that PL3 induced the reductions of cyclins A and B, and Cdk1 in PL3-treated K562 cells (Fig. 5B). Due to a decrease in Cdk1, an increase in the Cdk inhibitor, P21, protein expression was

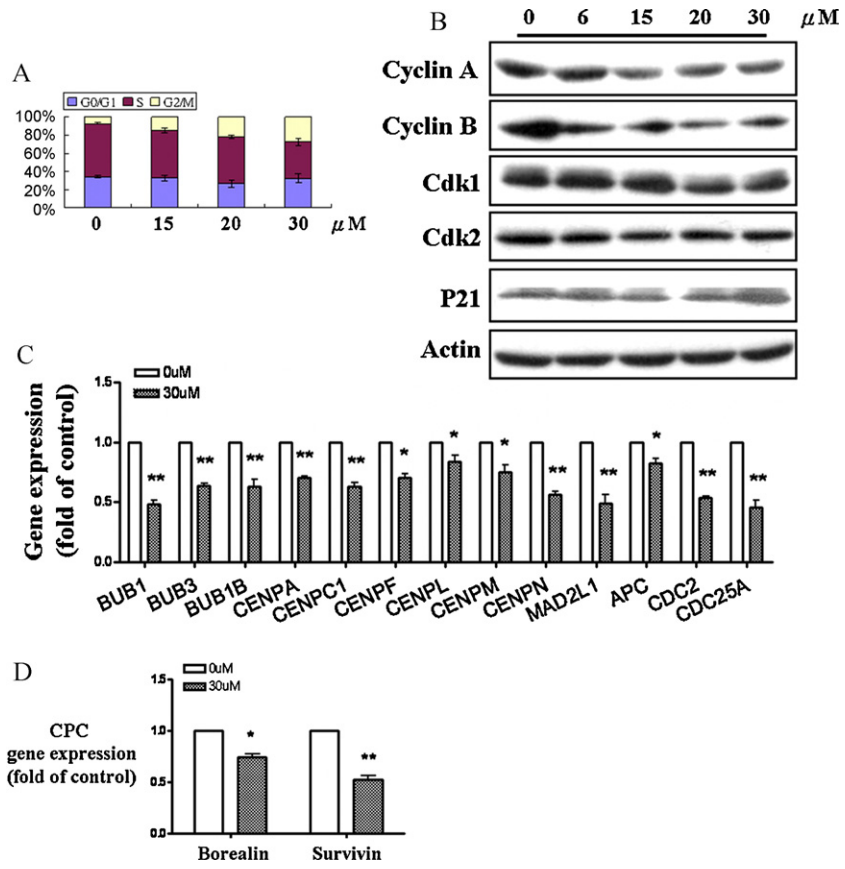

Fig. 5. Impacts of PL3 on mitotic checkpoint defects and G_2/M phase arrest. (A) Cell-cycle distribution (in percent) determined by flow cytometry. K562 cells were treated with the indicated concentrations of PL3 for 24 h and fixed with propidium iodide (PI) staining for the flow cytometric analysis. (B) K562 cells were treated with the indicated concentrations (0, 6, 15, 20, and 30 μM) of PL3 for 24 h, cells were harvested, and cell-cycle G_2/M phase regulation complex components, cyclin A, cyclin B, and Cdk1, were analyzed by Western blotting. (C) Mitotic spindle checkpoint-related gene expressions regulated by PL3-treated K562 cells were examined. (D) K526 cell chromosomal passenger complex (CPC) gene expression reduced by PL3 was determined after 24 h of exposure by a real-time PCR analysis. $^{*}p < 0.05$; $^{**}p < 0.01$ (t-test).

detected in PL3-treated K562 cells. Moreover, because of the loss of Aurora B in PL3-treated K562 cells and the roles of Aurora kinases in microtubules during chromosome movement and segregation, integrated spindle checkpoint gene expressions, such as those of the centromere protein family (involved in the spindle checkpoint function), were determined. It was observed that PL3 reduced gene expressions of the spindle checkpoint and mitotic spindle assembly checkpoint (about 20–50% reductions) in K562 cells (Fig. 5C). Based on the importance of Aurora B in spindle checkpoint stability, the impact of PL3 on chromosomal passenger complex (CPC) gene expressions was also determined (Fig. 5D). These observations were found to be consistent with Aurora B dysfunction in PL3-treated K562 cells.

3.6. PL3 reverses Imatinib resistance of CML T315I cells with combination treatment

T315I-mutated CML cells are well known to be resistant to Imatinib, which is effective in treating patients with leukemia who carry a different mutation (Hanko et al., 2008). The T315I mutation of Bcr-ABL is clinically significant, as CML cells harboring this mutation are insensitive to Imatinib and other Bcr-ABL-targeted drugs. We investigated the effect of PL3 on T315I-mutated Bcr-ABL$^+$ BA/F3 cells as PL3 was active in leukemia cells by reducing Aurora B expression. T315I-mutated Bcr-ABL$^+$ cells were incubated with the gradient concentrations of PL3 for 24 h, and cell viability was later determined by an MTT assay, as shown in Fig. 6A. It was demonstrated that PL3 also induced cytotoxicity in T315I-mutated Bcr-ABL$^+$ cells (with an IC_{50} value of 30 μM). Next, the combined treatment with PL3 and Imatinib in T315I-mutated Bcr-ABL$^+$ cells was examined. A non-cytotoxic concentration of PL3 (9 μM for T315I$^+$ cells) was used to combine with an increasing concentration of Imatinib. The results revealed that PL3 significantly reversed the Imatinib-resistance of T315I-mutated Bcr-ABL$^+$ cells compared to treatment with only Imatinib (Fig. 6B). The obtained data suggest that PL3 is a promising compound capable of killing T315I-mutated Bcr-ABL$^+$ cells through combined treatment.

4. Discussion

Recent studies demonstrated that PI3K-AKT and Aurora B are promising targets for anticancer drug development. In the present study, we first investigated the effect of the natural compound, PL3, on cancer cells and mainly focused on leukemia K562 cells, and we subsequently tested it on other cell types including leukemia HL-60 and Molt-4 cells, and solid-tumor SW620, A549, and GBM8401 cells to confirm its anticancer properties and possible molecular mechanisms. Herein, it was observed that PL3 was cytotoxic to the all six cancer cell lines with IC_{50} values in the range of 15–140 μM. It was also found that PL3-induced apoptosis partly occurred through a caspase-dependent pathway in K562, SW620, and GB8401 cells. These were because the above-mentioned six cell lines originate from different cancers and have various molecular profiles, such as p53$^-$, p53$^+$, and p53 mutations. It is necessary to discover anticancer drugs to treat cancer cells regardless of their molecular profile. PL3 reduced Aurora B expression in the six cell lines. According to the crosstalk between the PI3K-AKT pathway and Aurora B kinase, and the fact that the PI3K-AKT pathway is highly conserved

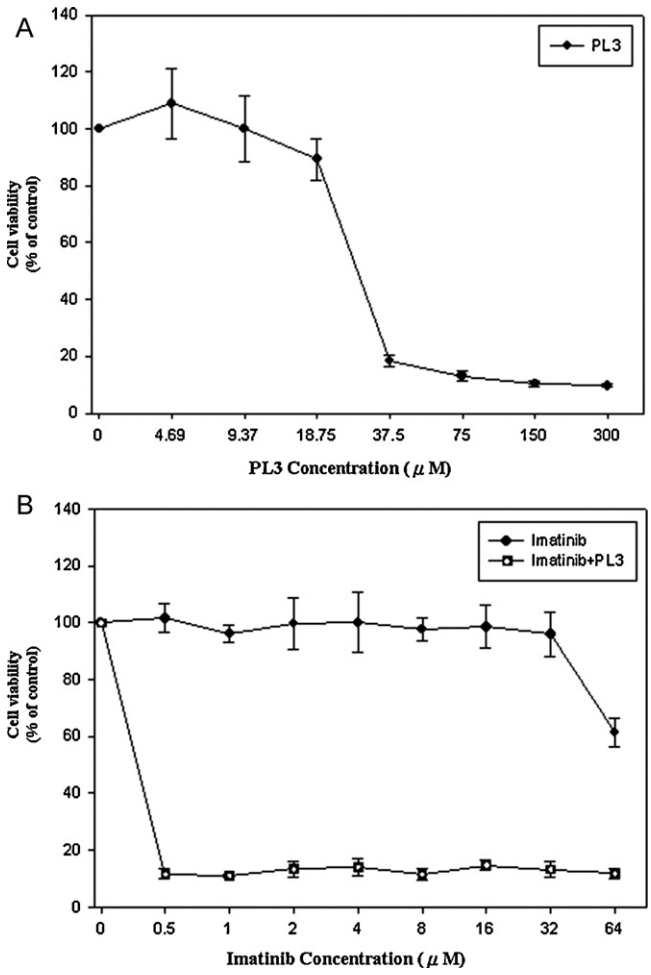

Fig. 6. Combined treatment with PL3 and Imatinib in T315I-mutated Bcr-ABL$^+$ cells. (A) T315I-mutated Bcr-ABL$^+$ cells were treated with 0–300 μM PL3 alone for 24 h, and the 50% inhibitory concentration (IC_{50}) value was determined by an MTT assay. (B) A non-cytotoxic concentration (9 μM for T315I cells) of PL3 and the indicated concentrations of Imatinib were combined to treat T315I-mutated Bcr-ABL$^+$ cells for 24 h, and the IC_{50} value was calculated.

in cancer cells, it is reasonable to identify the potential inhibitory effect of PL3 on PI3Ks.

Through a molecule-protein docking program, PL3 was predicted to potentially bind to the active site of P85α, a PI3K subunit. In addition, the phosphorylation status of both PI3K P85α^{tyr508} and AKT^{ser473} was demonstrated by immunoblotting with phospho-specific antibodies. Blockage of the PI3K-AKT pathway induced apoptosis through activating apoptotic stimuli in cancer cells. PL3 bound to PI3K P85α, reduced the phosphorylation status of P85α, and affected its ability to phosphorylate downstream signaling effectors including AKT. An effective approach in anticancer therapy is to inhibit the activities of kinases by blocking active sites towards the substrate. PL3 exhibited potential binding affinity with the PI3K subunit, P85, and significantly inhibited PI3K-AKT activities.

It was demonstrated that both AKT and Aurora kinases are important targets for cancer chemotherapy. When investigating the correlation between the PI3K-AKT pathway and Aurora B kinase expression, PI3K inhibitor treatment confirmed the regulatory effect between PI3K activity and Aurora B expression. In addition to inhibiting Aurora B expression, PL3 also decreased Aurora B activity of maintaining the integrity of the spindle checkpoint and histone H3 Ser10 phosphorylation. CPC is an essential component in histone H3 Ser10 phosphorylation and plays key regulatory roles of

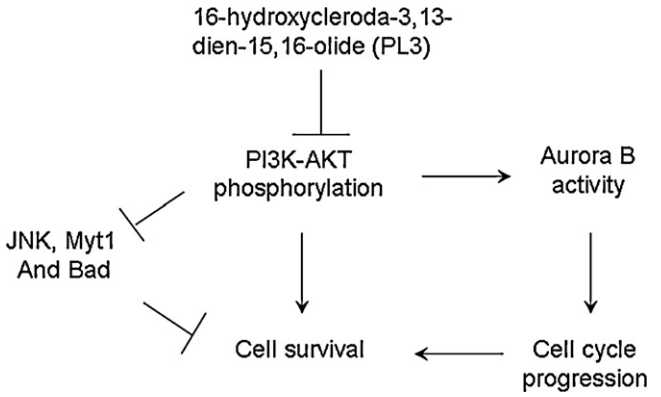

Fig. 7. The predicted mechanism of PL3's action against cancer cells. PL3 may bind with PI3K P85 and affect at least two of its downstream pathways: (1) Aurora B and spindle assemble checkpoint integrity for normal mitosis and (2) activation of JNK, Myt1, and other proapoptotic effectors leading to apoptosis.

chromosome segregation and cytokinesis, where its functions are connected to its localization (de la Barre et al., 2000; Frankevich et al., 2003). The complex is first localized to centromeres and later associates with the central spindle and midbody. With the reduction of Aurora B, CPC gene expressions were also reduced by PL3.

In the absence of survival signals, P21 was reactivated to inhibit Cdk–cyclin complex formation and cause cell-cycle arrest in the G_2/M phase (Kim and Chung, 2002). This resulted in chromosome segregation defects during cell division, which are involved in blocking cell mitosis and genomic instability. When investigating the possible apoptotic mechanism, it was observed that PL3 caused dephosphorylation of PI3K-AKT and activated apoptosis regulators, including the MAPK-JNK pathway, by increasing its phosphorylation status. Furthermore, PL3 also significantly activated the tumor-suppressor genes, TSC1 and Myt1, and gene expressions of the proapoptotic effectors, Bad and FoxO3, in the absence of PI3K-AKT activation of K562 cells (Fig. 7).

Concentrations of PL3 were relatively high and cytotoxic. On the basis of its apoptosis-inducing property, PL3 can be used as an initial chemical scaffold. In addition, derivatives of this compound that can be applied in a clinical setting can also be screened. Furthermore, accumulated evidence suggests that Aurora kinase inhibitors are applicable in acute myeloid leukemia (AML) and Imatinib-resistant chronic myeloid leukemia (CML), particularly the T315I mutation (Acquaviva et al., 2010). PL3 significantly reversed the drug-resistance of Bcr-ABL T315I-positive cells to Imatinib by slashing the necessary concentration for inducing cytotoxicity. Elucidating the mechanism requires further investigation and study. Altogether, it was discovered that the PI3K-AKT pathway can be a regulator of Aurora B which is involved in cell-cycle regulation and cell-fate decisions in cancer cells. The outcomes of the present study provide a new natural compound that influences cancer cell proliferation and a deficiency in the mitosis checkpoint. Further, it was also observed that DNA-repair proteins prohibited cells from recovering from apoptosis-induced DNA damage. The obtained results indicate that PL3 can be considered for targeted chemotherapy as well as combined with other clinical medications.

Funding source

This work was supported by a grant from Kaohsiung Medical University, Taiwan.

Conflict of interest

None declared.

Appendix A. Supplementary data

Supplementary data associated with this article can be found, in the online version, at doi:10.1016/j.tox.2011.04.004.

References

Acquaviva, C., Gelsi-Boyer, V., Birnbaum, D., 2010. Myelodysplastic syndromes: lost between two states? Leukemia 24, 1–5.

Alessi, D.R., Caudwell, F.B., Andjelkovic, M., Hemmings, B.A., Cohen, P., 1996. Molecular basis for the substrate specificity of protein kinase B; comparison with MAPKAP kinase-1 and p70 S6 kinase. FEBS Lett. 399, 333–338.

Alessi, D.R., Deak, M., Casamayor, A., Caudwell, F.B., Morrice, N., Norman, D.G., Gaffney, P., Reese, C.B., MacDougall, C.N., Harbison, D., Ashworth, A., Bownes, M., 1997. 3- Phosphoinositide-dependent protein kinase-1 (PDK1): structural and functional homology with the Drosophila DSTPK61 kinase. Curr. Biol. 7, 776–789.

Arcaro, A., Wymann, M.P., 1993. Wortmannin is a potent phosphatidylinositol 3-kinase inhibitor: the role of phosphatidylinositol 3,4,5-trisphosphate in neutrophil responses. Biochem. J. 296 (Pt 2), 297–301.

Chang, F.R., Hwang, T.L., Yang, Y.L., Li, C.E., Wu, C.C., Issa, H.H., Hsieh, W.B., Wu, Y.C., 2006. Anti-inflammatory and cytotoxic diterpenes from formosan *Polyalthia longifolia* var. pendula. Planta Med. 72, 1344–1347.

de la Barre, A.E., Gerson, V., Gout, S., Creaven, M., Allis, C.D., Dimitrov, S., 2000. Core histone N-termini play an essential role in mitotic chromosome condensation. EMBO J. 19, 379–391.

Dieterle, A., Orth, R., Daubrawa, M., Grotemeier, A., Alers, S., Ullrich, S., Lammers, R., Wesselborg, S., Stork, B., 2009. The Akt inhibitor triciribine sensitizes prostate carcinoma cells to TRAIL-induced apoptosis. Int. J. Cancer 125, 932–941.

Engelman, J.A., Luo, J., Cantley, L.C., 2006. The evolution of phosphatidylinositol 3-kinases as regulators of growth and metabolism. Nat. Rev. Genet. 7, 606–619.

Frankevich, V., Zhang, J., Dashtiev, M., Zenobi, R., 2003. Production and fragmentation of multiply charged ions in 'electron-free' matrix-assisted laser desorption/ionization. Rapid Commun. Mass Spectrom. 17, 2343–2348.

Fruman, D.A., Meyers, R.E., Cantley, L.C., 1998. Phosphoinositide kinases. Annu. Rev. Biochem. 67, 481–507.

Gharbi, S.I., Zvelebil, M.J., Shuttleworth, S.J., Hancox, T., Saghir, N., Timms, J.F., Waterfield, M.D., 2007. Exploring the specificity of the PI3K family inhibitor LY294002. Biochem. J. 404, 15–21.

Gully, C.P., Zhang, F., Chen, J., Yeung, J.A., Velazquez-Torres, G., Wang, E., Yeung, S.C., Lee, M.H., 2010. Antineoplastic effects of an Aurora B kinase inhibitor in breast cancer. Mol. Cancer 9, 42.

Hanko, V.P., Rohrer, J.S., Liu, H.H., Zheng, C., Zhang, S., Liu, X., Tang, X., 2008. Identification of tobramycin impurities for quality control process monitoring using high-performance anion-exchange chromatography with integrated pulsed amperometric detection. J. Pharm. Biomed. Anal. 47, 828–833.

Kim, D., Chung, J., 2002. Akt: versatile mediator of cell survival and beyond. J. Biochem. Mol. Biol. 35, 106–115.

Liu, X., Shi, Y., Woods, K.W., Hessler, P., Kroeger, P., Wilsbacher, J., Wang, J., Wang, J.Y., Li, C., Li, Q., Rosenberg, S.H., Giranda, V.L., Luo, Y., 2008. Akt inhibitor a-443654 interferes with mitotic progression by regulating aurora a kinase expression. Neoplasia 10, 828–837.

Liu, P., Cheng, H., Roberts, T.M., Zhao, J.J., 2009. Targeting the phosphoinositide 3-kinase pathway in cancer. Nat. Rev. Drug Discov. 8, 627–644.

Osterberg, T., Norinder, U., 2001. Prediction of drug transport processes using simple parameters and PLS statistics. The use of ACD/logP and ACD/ChemSketch descriptors. Eur. J. Pharm. Sci. 12, 327–337.

Rakvag, T.T., Klepstad, P., Baar, C., Kvam, T.M., Dale, O., Kaasa, S., Krokan, H.E., Skorpen, F., 2005. The Val158Met polymorphism of the human catechol-O-methyltransferase (COMT) gene may influence morphine requirements in cancer pain patients. Pain 116, 73–78.

Scheid, M.P., Lauener, R.W., Duronio, V., 1995. Role of phosphatidylinositol 3-OH-kinase activity in the inhibition of apoptosis in haemopoietic cells: phosphatidylinositol 3-OH-kinase inhibitors reveal a difference in signalling between interleukin-3 and granulocyte-macrophage colony stimulating factor. Biochem. J. 312 (Pt 1), 159– 162.

Schmitt, C.A., Fridman, J.S., Yang, M., Baranov, E., Hoffman, R.M., Lowe, S.W., 2002. Dissecting p53 tumor suppressor functions in vivo. Cancer Cell 1, 289–298.

Shih, Y.T., Hsu, Y.Y., Chang, F.R., Wu, Y.C., Lo, Y.C., 2010. 6-Hydroxycleroda-3,13-dien-15,16-olide protects neuronal cells from lipopolysaccharide-induced neurotoxicity through the inhibition of microglia-mediated inflammation. Planta Med. 76, 120–127.

Takashima, A., Noguchi, K., Michel, G., Mercken, M., Hoshi, M., Ishiguro, K., Imahori, K., 1996. Exposure of rat hippocampal neurons to amyloid beta peptide (25-35) induces the inactivation of phosphatidyl inositol-3 kinase and the activation of tau protein kinase I/glycogen synthase kinase-3 beta. Neurosci. Lett. 203, 33–36.

Varticovski, L., Druker, B., Morrison, D., Cantley, L., Roberts, T., 1989. The colony stimulating factor-1 receptor associates with and activates phosphatidylinositol-3 kinase. Nature 342, 699–702.

Yang, J.M., Chen, C.C., 2004. GEMDOCK: a generic evolutionary method for molecular docking. Proteins 55, 288–304.

Yano, H., Nakanishi, S., Kimura, K., Hanai, N., Saitoh, Y., Fukui, Y., Nonomura, Y., Matsuda, Y., 1993. Inhibition of histamine secretion by wortmannin through the blockade of phosphatidylinositol 3-kinase in RBL-2H3 cells. J. Biol. Chem. 268, 25846–25856.

Yao, J.E., Yan, M., Guan, Z., Pan, C.B., Xia, L.P., Li, C.X., Wang, L.H., Long, Z.J., Zhao, Y., Li, M.W., Zheng, F.M., Xu, J., Lin, D.J., Liu, Q., 2009. Aurora-A down-regulates IkappaBalpha via Akt activation and interacts with insulin-like growth factor-1 induced phosphatidylinositol 3-kinase pathway for cancer cell survival. Mol. Cancer 8, 95.